Electrical Power and Energy Systems 153 (2023) 109390

Contents lists available at ScienceDirect

International Journal of Electrical Power and Energy Systems

journal homepage: www.elsevier.com/locate/ijepes

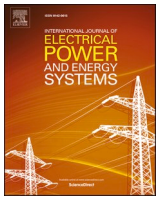

Development of the equivalent Great Britain 36-zone power system for frequency control studies

Rasoul Azizipanah-Abarghooee [a], Mostafa Malekpour [a], Mazaher Karimi [b,*], Vladimir Terzija [c]

[a] Green Energy and Mobility Department, RINA Tech UK Ltd, Manchester, UK
[b] School of Technology and Innovations, University of Vaasa, Vaasa, Finland
[c] School of Engineering, Merz Court E4.41, Newcastle University, UK

ARTICLE INFO

Keywords:
Frequency control
Dynamic model
Modal analysis
Rate of change of frequency
Small-signal analysis
Time-domain simulations

ABSTRACT

This paper presents a dynamic model of the equivalent Great Britain (GB) 36-zone power system, which can be used for reliable and realistic assessment of emerging load frequency control mechanisms. Flexible architecture of the presented dynamic test system permits a broad range of security of supply and small-signal stability studies for design of future power grids. It can be particularly useful for academic research, but also for undertaking feasibility studies in power industries. The proposed dynamic test system, which is obtained through network reduction of the original full-scale GB transmission power system developed by National Grid Electricity System Operator (NGESO) Company, provides detailed information about the GB power system. In this regard, the required data and modelling approaches to develop the 36-zone system are provided in detail. The presented dynamic test system represents the system topology, impedance characteristics and electromechanical oscillations of the original GB power system however, it is not an exact equivalent of the master GB system. Illustrative dynamic models of the key system components, including synchronous generators, automatic voltage regulators, power system stabilizers, hydro and steam turbines models along with speed governing systems are presented. Dynamic behavior of 36-zone test system in response to infeed loss contingencies is investigated. Particularly, the impact of changes in the system inertia on the system electromechanical modes is examined using the modal analysis approach. In this context, the mode shape concept is employed to determine dominant generators and contribution of different zones in the low frequency oscillations. Moreover, time-domain simulations are undertaken to validate the modal analysis results. Additionally, the condition of different zones from the viewpoint of frequency nadir and maximum rate of change of frequency for various contingencies and extreme cases are examined.

1. Introduction

Power systems frequency is a reliable indicator to monitor instantaneous balance between power generation and power consumption [1]. Many researches have revealed that without sufficient fast frequency reserves, future low inertia power systems experience large prolonged frequency excursions [2,3]. For example, frequency control in the Great Britain (GB) power system will become more challenging as the generation mix changes towards higher levels of non-synchronous inverter-based resources (IBRs) [3]. According to Gone Green 2020 scenario, the GB power system behavior is principally driven by increasing penetration of inertia-less IBRs and European Union interconnectors using high voltage direct current (HVDC) links [3]. Traditional analysis of frequency has been done at a purely national level considering a total inertia for whole system. However, it is to be noticed that the regional inertia's impact on system stability subjected to small disturbance as well as large disturbance contingencies become a vital challenge due to IBRs geographically distributed in future power grids. Moreover, the delivery of frequency response occurs in discrete localized actions across the GB system [3]. Therefore, in addition to any frequency response resulting in oscillations following the infeed loss in a low inertia system at the point of frequency recovery, the low frequency oscillations (LFO) can be also observed during that recovery period. This would have a different nature across power grids as the power transfers supporting an energy balance excite inter-area modes [4]. In low-inertia systems, it can be examined to which extent the loss of the fast power responses

* Corresponding author.
E-mail address: mazaher.karimi@uwasa.fi (M. Karimi).

https://doi.org/10.1016/j.ijepes.2023.109390
Received 17 April 2023; Received in revised form 30 May 2023; Accepted 21 July 2023
Available online 25 July 2023

provided by system inertia may be mitigated by fast frequency responses from different ancillary service providers. These services have the potential to excite the inter-area modes within a transmission system and their control and effects of deployment need to be understood against the network impacted [5,6,7]. The UK's frequency response services, their technical requirements and costs are provided in [8].

After power imbalance contingencies, there is a potential risk for system instability when inter-area modes with insufficient damping are excited [9]. It is also possible for local rate of change of frequency (RoCoF) to substantively differ from the equivalent national level. To avoid such scenarios, load frequency control studies should be done by investigating modal analysis, mode shape concept, time-domain simulation, as well as frequency nadir and RoCoF metrics through multiple study cases. These types of analyses which are commonly employed by transmission system operators (TSOs) in control center rooms improve the situational awareness. This would provide a visualization of the frequency and damping of dominant electromechanical modes, their mode shapes, frequency response, RoCoF, and also finding worse case scenarios in terms of minimum frequency nadir and maximum RoCoF.

Generally speaking, both the parameters and types of the dynamic modeling should be accessible for all power system components for conducting the practical dynamic analysis. On one hand, each electric company has its own dynamic types and parameters for its power system devices. In the other hand, it is noteworthy that several IEEE power test systems which are available for steady state analysis suffer from lack of dynamic models. In this regard, a few IEEE standards note that practical test systems are proposed in [10,11]. There are several cases where researchers are enforced to select their own dynamic models which lead to inconsistency between them [12]. It is difficult to validate studies on practical test system because there is no realistic benchmark test system with dynamic modellings available for such systems.

In this paper, a benchmark test system for a typical transmission network is developed which is suitable for dynamic evaluation of existing and future load frequency control mechanisms. Resulting from the geographic position of the Great Britain, the GB power system can be considered as a relatively small system, however connected over HVDC interconnectors to surrounding larger power systems. That is why this test system can be of particular importance for validating new smart grid concepts. This study provides further modifications of the 36-zone test system as provided by National Grid Electricity System Operator (NGESO) to the researchers. This would improve the inter-area, frequency nadir, and RoCoF evaluations using this reduced model of the GB power system [13]. The dynamic parameters for a sixth-order and fifth-order round and salient pole rotors' synchronous machine models, automatic voltage regulators (AVRs), power system stabilizers (PSSs) are defined. Moreover, load frequency control mechanisms using hydro and steam speed governing systems are developed in detail as well as turbines dynamic models. The provided system is configured using illustrative structural characteristics and the test system is implemented in DIgSILENT PowerFactory software and can also be modeled in other software packages like RSCAD/RTDS. Therefore, the test system users can readily adjust its characteristics to satisfy their preferences [14,15], or to study other problems like transient voltage stability that have not yet been investigated on this power system. Therefore, the following contributions are made in this study:

- A dynamic benchmark power system is proposed based on the equivalent GB 36-zone power system
- Hydro and steam speed governing systems are designed for load frequency control mechanism
- Dominant generators for different inter-area modes are determined through modal analysis
- Characteristics of the low frequency oscillations are investigated for three slowest inter-area modes
- Load frequency control performance is validated through time domain simulations for various contingencies

The 36-zone power system differs in purpose and scale from previously developed test systems [16,17]. This is a reduced model which has sought to preserve in its reduction known aspects of the inter-area dynamics of the GB transmission system. In fact, this test system is a new version of publicly available network topology data as found within NGESO's Electricity Ten Year Statements [18], which is equipped with dynamic models for power plants. It was utilized in large-scale projects such as Enhanced Frequency Control Capability (EFCC) [13] Phoenix [19] and MIGRATE [20] projects, all run through collaboration between industry and university partners. Additionally, the proposed 36-Zone GB test system can be an optimal candidate for development and testing of novel solutions in the areas of power system dynamics and stability, protection and optimal exploitation of renewable energy sources. In general, the test system is optimal for testing of smart grid methods, tools and solutions, a number of which are discussed in this study. The exhibition of a combination of electromechanical local and inter-area modes, deployment of power oscillation damping controllers, evaluation of the small signal analysis results is achieved by comparing the modes characteristics and time-domain simulation results. This proposed dynamic benchmark test system provides a simulation platform to validate several power system studies.

This paper is organized as follows: Section 2 describes components of the 36-zone test system and their dynamic models. An illustrative application of the test system based on modal analysis is given in Section 3. Performance of the designed load frequency control mechanism is investigated in Section 4. Finally, the paper is concluded in Section 5.

2. Great Britain 36-Zone power system description

In this section, a general description of the proposed 36-zone test system is firstly provided. Afterwards, the developed approach for power stations modeling is presented.

2.1. The test system description

The single line diagram of 36-zone test system is depicted in Fig. 1 (a) where the zones are connected to each other's using 69 transmission lines at 400 kV voltage level. In each zone, the synchronous generators are connected to the zone 400 kV terminal through 33 kV/400 kV two-winding transformers with 17% short-circuit voltage. In this test system, the zones are enumerated from the south to the north. In addition, the geographical distribution of loads and their values are portrayed in Fig. 1 (b). The total system demand is about 40 GW which is mostly concentrated on the southern part of the country rather than the northern one. In particular, the lowest and highest amounts of loads range between 60 MW and 3,670 MW and are located in zone 31 (Northern area) and zone 8 (close to London), respectively. The voltage dependency of loads characteristics is represented by the polynomial ZIP model. The active power component P and reactive component Q are considered separately as follows [21]:

$$P = P_0\left(p_1\left(\frac{V}{V_0}\right)^2 + p_2\left(\frac{V}{V_0}\right) + p_3\right) \tag{1}$$

$$Q = Q_0\left(q_1\left(\frac{V}{V_0}\right)^2 + q_2\left(\frac{V}{V_0}\right) + q_3\right) \tag{2}$$

in which, P_0 and Q_0 denote the load active power and reactive power at an initial operating condition with bus voltage as V_0. The three terms in the right-hand sides of (1) and (2), model constant impedance (Z), constant current (I) and constant power (P) components of the loads, respectively [22]. The portion of each component is defined by coefficients p_1 to p_3 and q_1 to q_3 [23,24]. In the introduced test system, the coefficients p_1, p_2 and p_3 are set to 0.2, 0.35 and 0.45, correspondingly. This is also applicable for the loads reactive power components. Moreover, the frequency dependency of the loads active power is modelled by

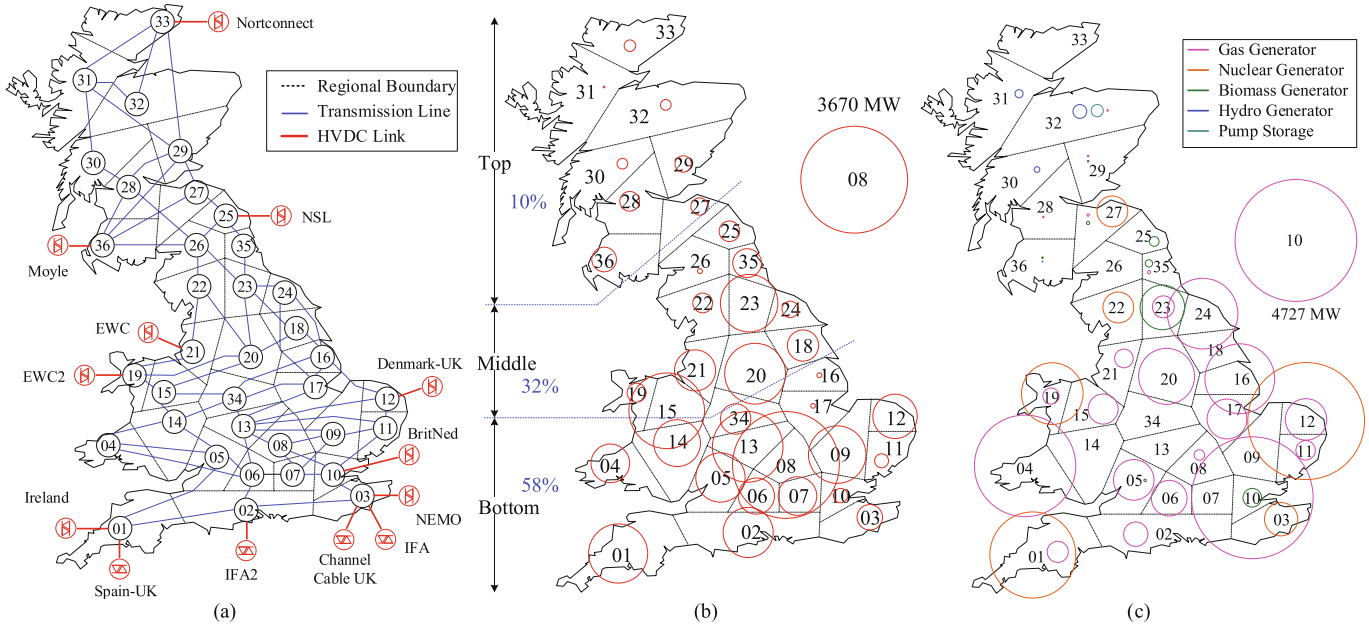

Fig. 1. 36-zone power system graphical representation: the geographical distributions of (a) the zones, (b) the system demand and (c) the power stations.

multiplying the polynomial model with a factor as follows [21]:

$$P = P_0\left(p_1\left(\frac{V}{V_0}\right)^2 + p_2\left(\frac{V}{V_0}\right) + p_3\right)\left(1 + k_{pf}\Delta f\right) \tag{3}$$

Where, Δf is the load bus frequency deviation with respect to the system nominal frequency. The parameter k_{pf}, that is commonly referred to load damping constant, typically ranged from 0 to 3 [24]. The load damping constant of 36-zone system is set to 1.0.

In the other hand, Fig. 1 (c) illustrates the diversity and types of the power stations in 36-zone system. In this test system, there are 41 power stations including 8 biomass, 30 gas, 6 nuclear, 4 hydro and a pump storage units. The hydro power stations are located in Scotland and the nuclear generations are placed at the UK shores. The next sub-section provides information regarding different components and controllers of these power plants.

2.2. The power station modelling

The main component of traditional power stations is synchronous generator (SG), which converts turbines mechanical power to electricity [20]. To derive the standard SG model, the relations of the coupled SG stator and rotor windings have been considered by transforming the variables of the windings into a rotor reference frame [21]. This standard 6th order SG model is illustrated in Fig. 2.

with one and two dampers in *d*-axis and q-axis, respectively [25]. However, the *q*-axis circuit of salient-pole SGs (in the hydro power stations) are characterized with one damper winding. In 36-zone test system, the SGs are directly interfaced with the power grid equations using the voltage behind reactance model [26,27]. In this study, the typical SGs' parameters have been selected, for both round and salient rotor SGs round, as are listed in Table 1 [28,29]. The base power for the impedances reported in Table 1 is the SG apparent power.

The block diagram of the power stations control system is plotted in Fig. 3(a). In the SGs excitation control scheme, an AVR tunes the exciting voltage of the SG according to its terminal voltage. The AVR control block is shown in Fig. 3 (b) [10]. It is a thyristor exciter with a transient gain reduction. The PSS controller defines an auxiliary signal to the AVR using SG rotor speed to provide additional damping torque for the SG [21]. The PSS block diagram which the researchers have selected to be utilized in this test grid is shown in Fig. 3 (c). Accordingly, the SG rotor

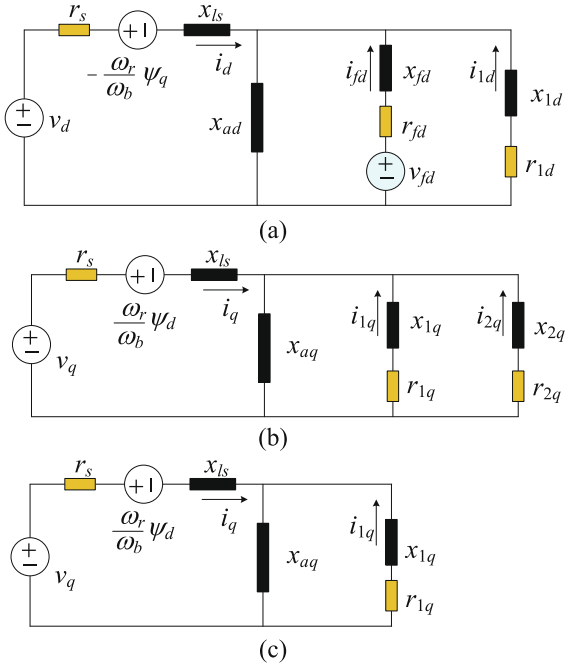

Fig. 2. The synchronous generator model: (a) d-axis equivalent circuit, (b) q-axis equivalent circuit for round rotor, (c) q-axis equivalent circuit for salient rotor.

speed deviation is firstly multiplied by a gain and then passed through a washout filter to remove steady-state frequency deviation. As shown, two cascading lead-lag filters are deployed to compensate the phase difference between the input signal of the AVR and electromagnetic torque of the SG. Finally, the output signal is restricted to a predefined value using a limiter.

On the other hand, the power plant mechanical systems are represented by the prime mover (PM) and the primary controller (PCO) blocks. The PM block models the turbine dynamics and the PCO controls the turbine output power. The PM and PCO block diagrams of the nuclear, gas or biomass power stations are depicted in Fig. 3 (d) [10]. The

Table 1
The SGs parameters for 36-zone test system [28].

Symbol	Description	Round	Salient	Unit
H	Inertia constant	5.6	7.5	*s*
rs	Stator resistance	0.003	0.0019	*p.u.*
xls	Stator leakage reactance	0.19	0.12	*p.u.*
rfd	Resistance of excitation winding	0.0012	0.0005	*p.u.*
xfd	Reactance of excitation winding	0.1532	0.2090	*p.u.*
r1d	Resistance of 1d-damper winding	0.0157	0.0168	*p.u.*
x1d	Reactance of 1d-damper winding	0.0778	0.1576	*p.u.*
r1q	Resistance of 1q-damper winding	0.0101	0.0164	*p.u.*
x1q	Reactance of 1q-damper winding	0.0931	0.1029	*p.u.*
r2q	Resistance of 2q-damper winding	0.0023	–	*p.u.*
x2q	Reactance of 2q-damper winding	0.8768	–	*p.u.*
xad	Mutual reactance of d-axis	1.6100	0.7300	*p.u.*
xaq	Mutual reactance of q-axis	1.6100	0.3600	*p.u.*

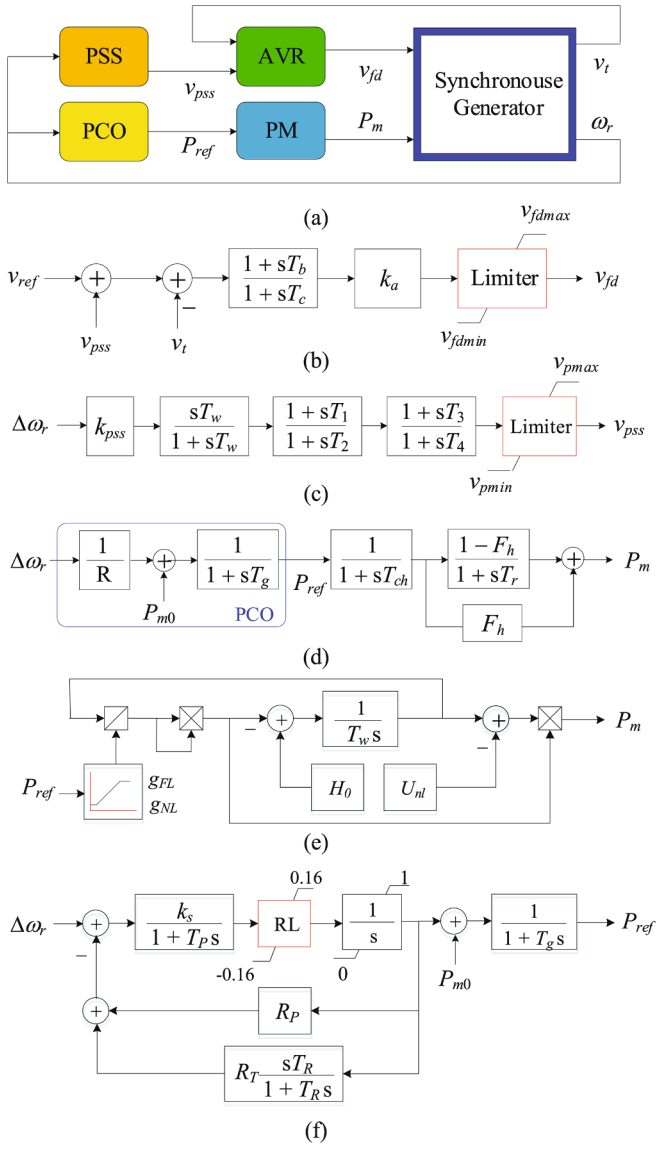

Fig. 3. Block diagrams of (a) the power stations control, (b) the AVR block, (c) the power system stabilizer-PSS block, (d) the primary controller and prime mover of the thermal stations-PCO and PM blocks, (e) the prime mover of the hydro stations- PM block, (f) the primary controller of the hydro stations-PCO block.

time constants of T_g and T_{ch} are pertinent to the PCO and the thermal turbine chest time delays, respectively. However, the largest time constant in this turbine model is T_r which shows the re-heater time delay. The F_h determines the high-pressure turbine contribution to generate power. The PCO adds a power deviation to the mechanical reference power based on the SG rotor speed variation with respect to rated speed [10]. In the case of the hydro power plants, the turbine non-linear model is illustrated in Fig. 3 (e). The parameter T_w, which is called water starting time, indicates the required time for water to accelerate in penstock from zero speed to U_0 for a head equals to H_0. The PCO block diagram related to the hydro-turbine is depicted in Fig. 3 (f). In this structure, to overcome the water inertia and stabilize the system, one transient droop equal to R_T is appended into the PCO model.

3. Illustrative Application: Modal analysis

3.1. Modal analysis results without considering power stations controllers

The SGs of the hydro power stations have been modelled as salient-pole rotor, while the rest of the 37 SGs are illustrated as round rotor SGs. Thus, the 36-zone system includes 242 state variables which are equal to the number of the calculated eigenvalues. These eigenvalues are shown in Fig. 4. The vertical axis represents the damped frequency of the modes in Hz. As the network has 41 SGs, there are 82 electromechanical complex modes. In Fig. 4, the red stars show the dominant generators (i.e., the units with participation factor greater than 0.5) for each group of eigenvalues. As can be seen from these results, the electromechanical modes can be divided into four groups. The damping time constant of these modes are reduced by moving from right to left in Fig. 4. In particular, the last left modes group has a time constant of 1.0 s, while this is 1.5 and 1.7 s for the second and third left groups. In other word, the damping of these modes takes less than 2 s, while this is 2.3 to 4 s for the right group. This type of mode is most significant to inter-area analysis due to their lower damping which will be investigated more than others hereinafter. It is observable that the dominant power plants for this mode group are based on this scenario condition and the assumed modelling above, 3 units of largest nuclear units, 4 stations from the largest gas units and all 4 hydro-electric units. Albeit the capacity of these four hydro turbines except one in zone 32 is negligible in comparison to the other 7 gas and nuclear power plants, the salient-rotor nature of these hydro-electric power stations makes their contribution in these modes more considerable. It has been investigated by the researchers that if these hydro-electric SGs were converted to round rotor SGs, the hydro-turbines of zones 30, 31 and 36 will not be the most dominant any more.

3.2. Modal analysis results considering power stations controllers

The electromechanical modes of 36-zone system by considering the excitation systems of the SGs are illustrated in Fig. 5. The results are provided for four different scenarios. The modes displayed in blue are identical with those of previously shown in Fig. 4. In the "With AVR" case identified by red color, all the 41 SGs are equipped with AVRs explained in section 2.2. It can be clearly seen that the AVRs reduce the modes damping which would lead to instability of the slowest mode. In the other two scenarios, it is assumed that all the SGs use a PSS excluding the gas unit in zone 1 and the biomass unit in zone 35. Comparing these scenarios reveals that increasing the PSSs lead filter time constant T_1 from 0.05 to 0.5 s would significantly increase the modes damping.

Interestingly, based on the dominant generators reported in Fig. 4, it can be inferred that it is not necessary to equip all 39 SGs in order to compensate the negative influence of the AVRs. To clarify this matter, the effect upon the electromechanical modes of 36-zone network, which gains support from only 11 PSSs located in the 11 dominant units specified in Fig. 4 (in the right map), for the slowest group of modes are shown in Fig. 6. It can be observed that damping of the slowest mode

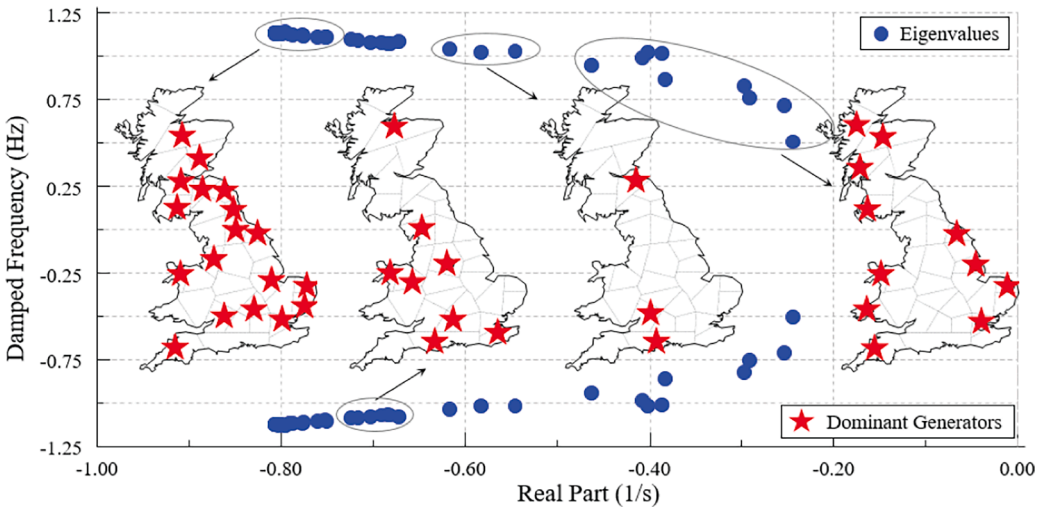

Fig. 4. 36-zone power system electromechanical modes with manual excitation control for the synchronous generators (the dominant generators are shown with stars).

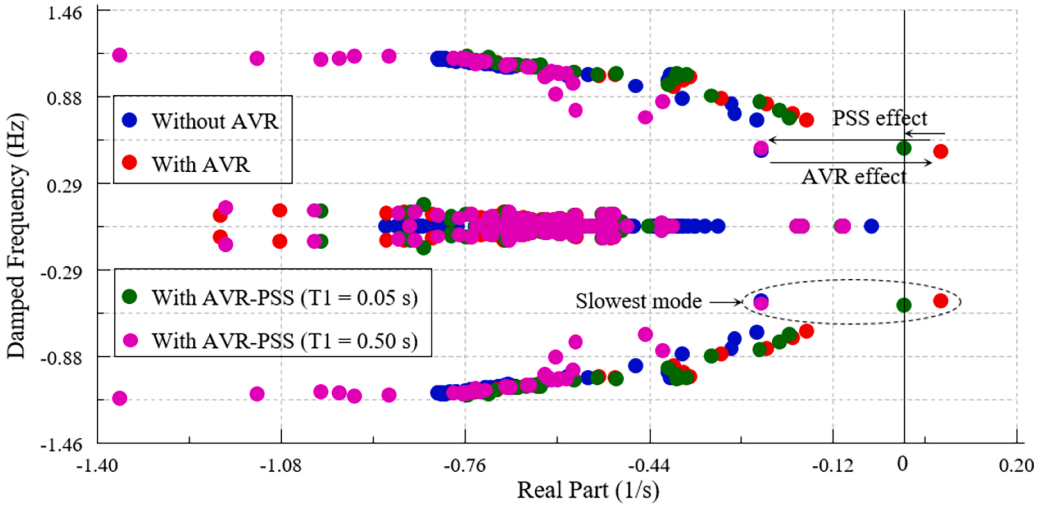

Fig. 5. Effect of AVR and PSS on the electromechanical modes of 36-zone power system.

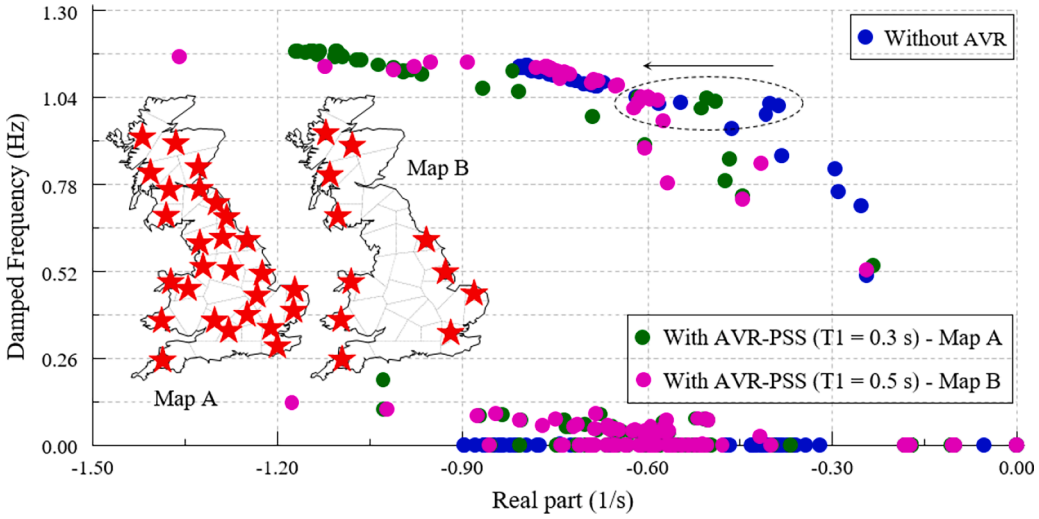

Fig. 6. Electromechanical modes of 36-zone power system for different numbers of generators equipped with PSS.

came back to the "Without AVR" scenario.

It is notable that turbines' dynamic model and their PCOs don't have a meaningful effect on damping of electromechanical modes [10]. In addition, the researchers have examined the use of SVC models also across the 36-zone network which whilst not materially influencing the faster modes, the damping and frequency of slower modes are decreased and increased, respectively. These changes are greater for the slower modes. Fig. 7 shows how the dominant generators are changed for the slowest modes before and after adding the dynamics of controlling devices. It is observable that the damping, and the damped frequency are respectively dropped down and grown for the slowest mode, while the dominant unit in both cases is the nuclear power of zone 1. In contrast, in general the damping of other three modes where the gas unit of zone 4 and the hydro plant of zone 32 are the dominant units increases after considering the assumed dynamics of control devices.

3.3. Modal analysis considering different system inertia levels

The un-damped natural frequency and damping ratio of a SG with inertia constant H, which is connected to an infinite bus, can be calculated as follows [21]:

$$\omega_n = \sqrt{\frac{\pi K_s}{H}} \tag{4}$$

$$\zeta = \frac{K_D}{4\sqrt{\pi f_b K_s H}} \tag{5}$$

where, K_D and K_s denote the damping torque coefficient and synchronizing torque coefficient, respectively. The system base frequency is indicated by f_b in Hz. Fig. 8 (a) shows the electromechanical modes in two more scenarios of increasing and decreasing the inertia of all SGs with the amount of 25% in comparison with the system base inertia H_b. The achieved eigenvalues for these two scenarios are displayed in magenta and blue colors in Fig. 8 (a). It is visible that the modes damping and frequency for all modes are significantly decreased by increasing the system inertia. This can be also justified by (4) and (5). Similar to Fig. 7, the system electromechanical slowest modes in just the dominant units are also provided (in dark green and black colors). Note that the *N*, *G* and *H* letters are used in the legend of Fig. 8 (a) to represent the nuclear, the gas and the hydro generators, respectively. As highlighted in the ellipsoid, the damping and its frequency of the faster modes don't vary considerably in case of inertia change. Fig. 8 (b) shows the slowest mode location change in case of increasing and decreasing the inertia of dominant units. The first and the second slowest modes are highlighted by two big ellipsoids. The locations of these two modes in case of the base inertia are bolded by the two squares. Locations of these two modes when the inertia of the four dominant generators vary, are almost equal to the case in which the inertia of all 41 SGs are changed.

3.4. Mode shapes of slow electromechanical modes

In order to precisely investigate the LFO oscillation in the 36-zone system, which is coming from interaction between the SGs rotors, the mode shape concept is deployed [10]. The mode shape is the observability or the normalized right eigenvector of a predefined state variable for a determinate eigenvalue [21]. The mode shape parameters related to the SGs rotor speed for the first, the second and the fifth slowest electromechanical modes are shown in Fig. 9 (a), (b) and (c), respectively. Accordingly, the amplitude of 37 power plants in the first two modes is greater than 0.1, so that these two modes are the system inter-area modes. In contrast, the amplitude of all SGs excluding the four hydroelectric units in the fifth mode shape is less than 0.1. Thus, this mode is a local one in the northern area. It is also observable from Fig. 9 (a) that the network is divided into two regions once the SG's rotor speed oscillation frequency is around 0.7 Hz and the SGs located in zones 1 to 10 swing against the other SGs. Similarly, it is clear-cut from Fig. 9 (b) that the network is divided into two regions once the SG's rotor speed oscillation frequency is around 0.8 Hz. However, in the case of the second mode the SGs in zone 1 swings with the similar direction to the SGs located in the northern area. Clearly, the four hydro power plants have a considerable contribution to the fifth slowest mode. In this case, the hydro unit of zone 31 swings against the other hydro plants.

4. Illustrative Application: Time domain analysis

4.1. Simulation results for loss of 1,720 MW generation

For the abnormal loss of generation up to 1,320 MW, which was went up to 1,800 MW from April 2014, the maximum frequency deviation (pertain to frequency nadir point) should be limited to 0.8 Hz and needs to be restored to 49.5 Hz within 60 s [25]. The nature of the GB network reduction to reach 36-zone system is to aggregate generation units, with similar energy resource, into a single "effective unit", within a given zone. In this regard, the biomass of zone 23 with the capacity of 1,720 MW is disconnected from the grid for illustration, however, it may not represent an actual physical condition of credible largest loss in the actual GB transmission system in that area. The frequencies of the gas generators in zones 23 and 35, the nuclear in zone 1 and hydro unit in zone 32 are portrayed in Fig. 10 (a). Moreover, their RoCoFs are plotted

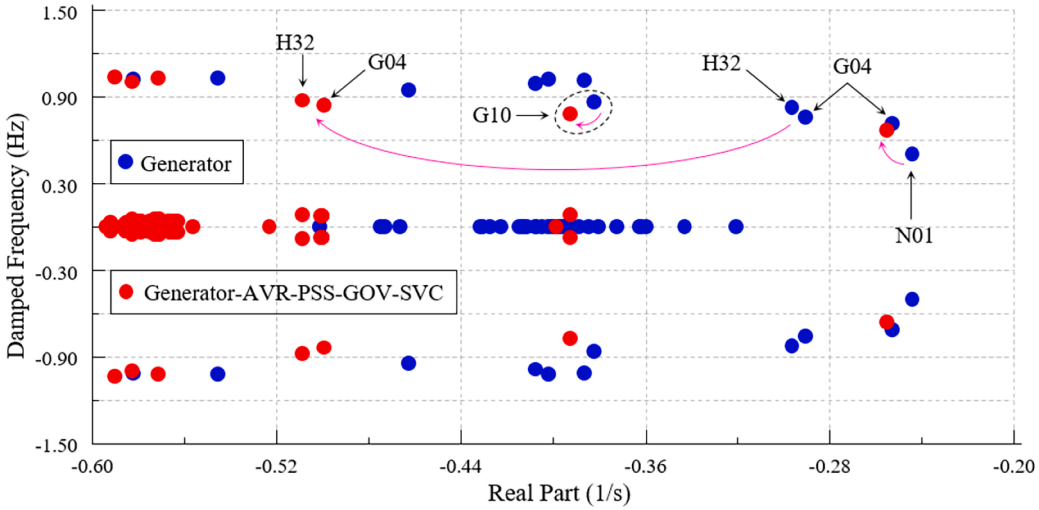

Fig. 7. Dominant generators in the slow electromechanical modes of 36-zone power system.

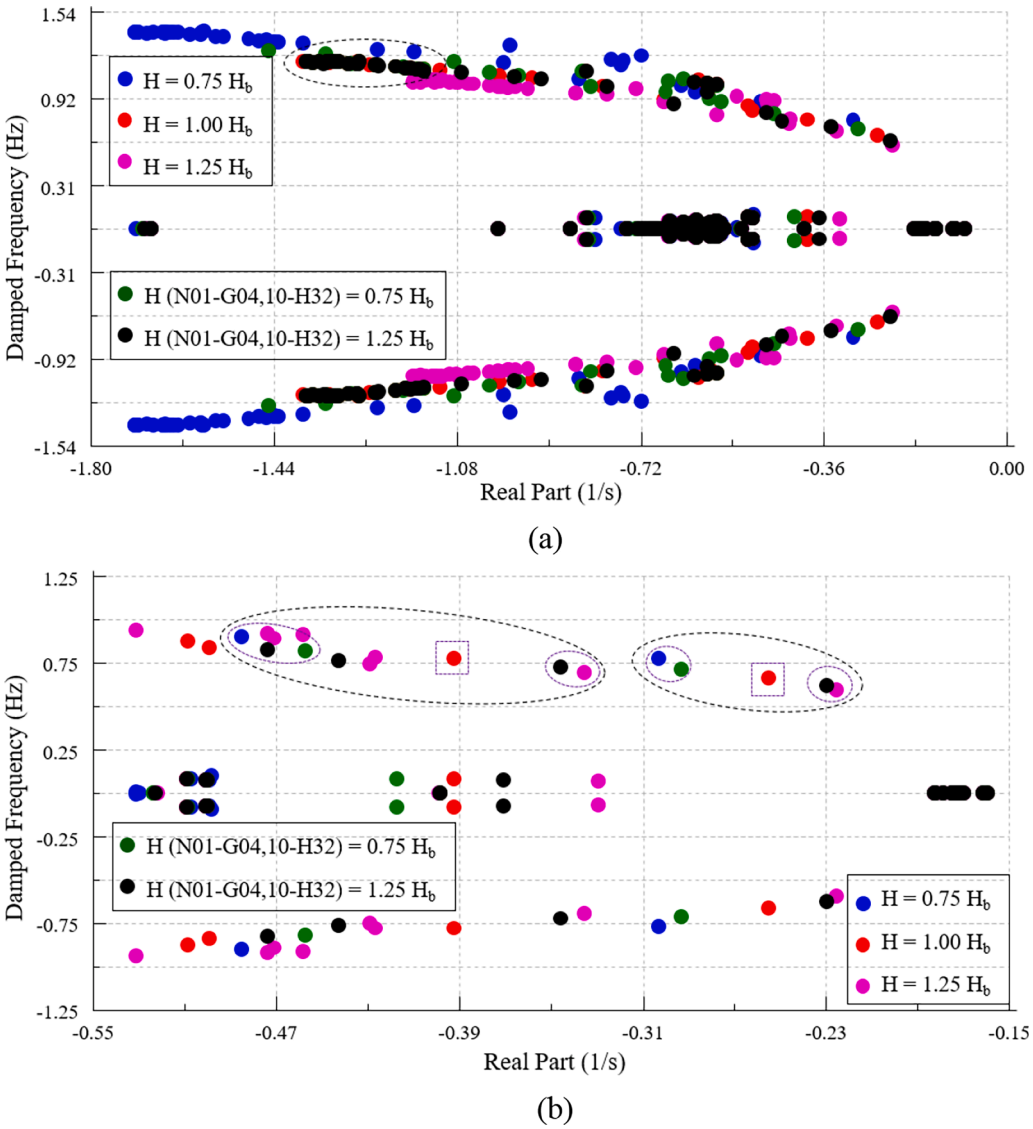

Fig. 8. 36-zone power system electromechanical modes: (a) the effect of generators inertia on modes and (b) the effect of generators inertia on slow modes.

in Fig. 10 (b). The center of inertia (COI) system frequency and its gradient are also provided in Fig. 10. It can be seen that the gas power plants in zones 23 and 35 as well as the hydro unit in zone 32 experience larger frequency gradients than the nuclear power in zone 1 due to their short distance to the faulted zone. On the other hand, the oscillations amplitude of the nuclear unit shows a poor damping characteristic against those of the other in question generators. The maximum RoCoF is corresponded to the gas generating unit in zone 23 with the amount of 0.5 Hz/s. Also, the worst frequency nadir is around 49.8 Hz. The steady-state frequency drop is almost 0.1 Hz.

4.2. Loss of 2400 MW generation in zone 27

As a significant loss of generation close to the 36-zone bottleneck, the nuclear unit of zone 27 generating 2400 MW is disconnected from the grid. The frequency and RoCoF variations pertinent to the gas units in zones 1 and 19, the biomass unit in zone 10 and hydro generator in zone 32 are illustrated in Fig. 11. It can be observable that the hydro generator oscillates more than other units through time due to its shorter distance to the fault location. It is clear-cut that gas unit 1 and hydro generator swings against each other as it was expected based on the mode shapes shown in Fig. 9 (a). Additionally, it can be concluded that the nearer the disturbance is, the faster the zone response is. In the other words, it is equivalent to the larger RoCoF values and vice versa. The maximum amount of RoCoF is pertinent to the gas generator in zone 19 which is about 1.2 Hz/s. The steady state frequency deviation is slightly greater than 0.1 Hz in this case. Furthermore, the disturbance location influences the frequency response of power systems and subsequently the EFCC project strategy for coordinating the fast frequency responses. Also, it is worth mentioning that every protection relay will see a different frequency gradient, depending on its distance to the event. In this context, the larger gradients can be indication for near or far the event location.

4.3. Frequency control performance assessment results

Following the results provided in the previous sections, the assessment results by conducting 18 different loss of generations are illustrated in Figs. 12 and 13. The frequency control performance metrics, i.e. the frequency nadir, maximum RoCoF and the steady-state frequency measured in zone 1 are reported in Fig. 12. In this case, the lowest frequency nadir and the maximum RoCoF are related to the loss of nuclear power plant located in zone 19. The bars shown in Fig. 13 report the in-question frequency metrics measured in zone 27. Similar to the previous

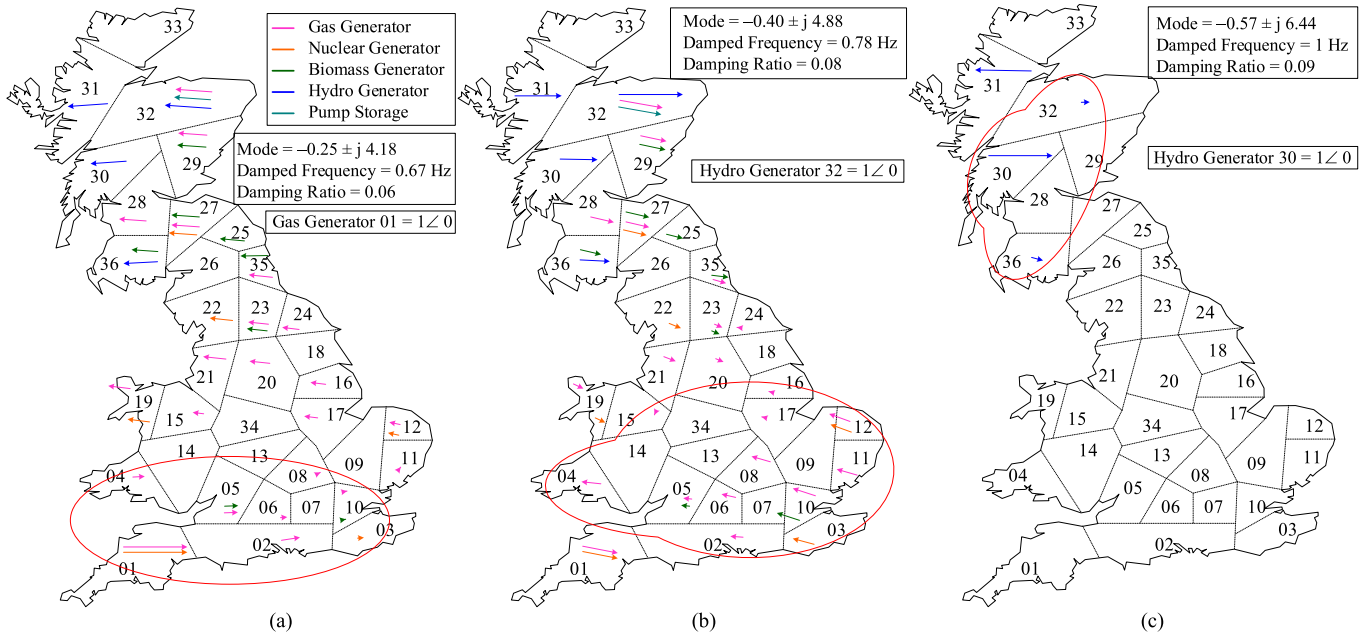

Fig. 9. Mode shapes pertinent to (a) the first; (b) the second and (c) the fifth slowest electromechanical modes.

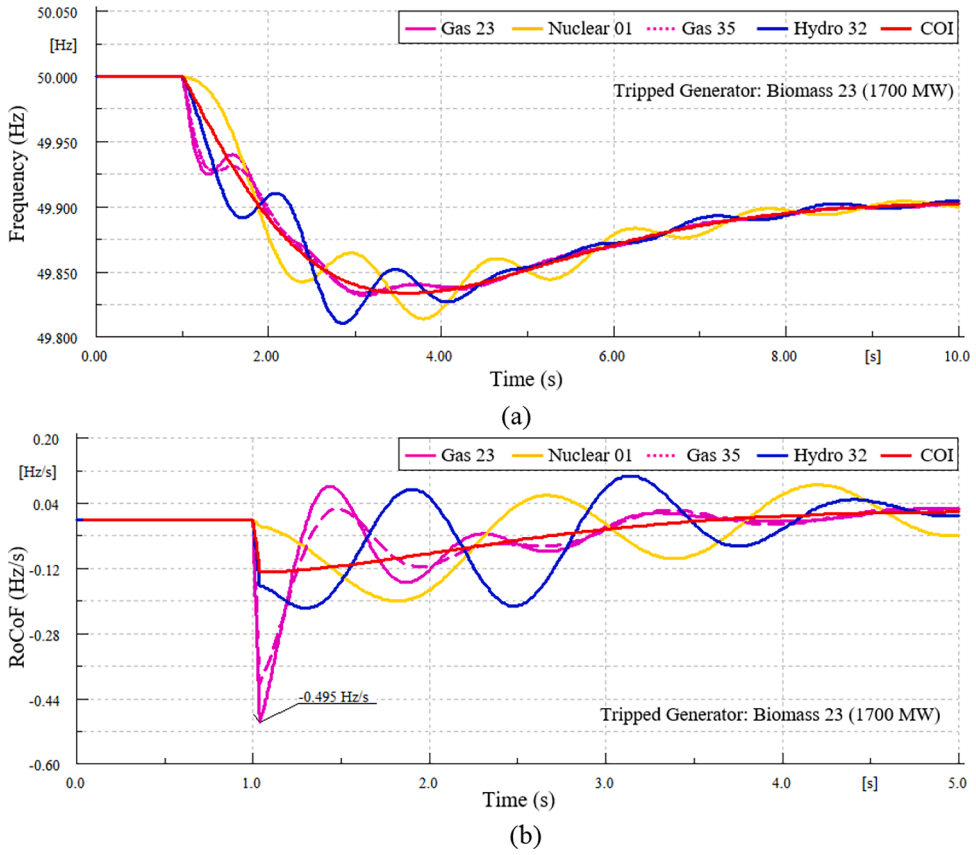

Fig. 10. 36-zone system frequency response to loss of 1700 MW generation: (a) the generators frequency and (b) the generators RoCoF.

measurements, loss of nuclear unit in zone 19 results in the lowest frequency nadir, however, it is not the case for the maximum RoCoF.

In order to get better insight into the relationship between the frequency control metrics with loss of generation size, the achieved minimum frequency nadir and the maximum RoCoF for distinct infeed loss contingencies, ranged from 1300 MW to 2400 MW, are provided in Fig. 14. The vertical axis represents the tripped generators along with their power generation in MW. The labels on the bars show the location of the corresponding extremum frequency metric. For the sake of comparison, the COI metrics are also provided in Fig. 14. It can be seen that the local frequency nadir values are always lower than the nation level COI frequency nadir. Moreover, the difference between the local and the

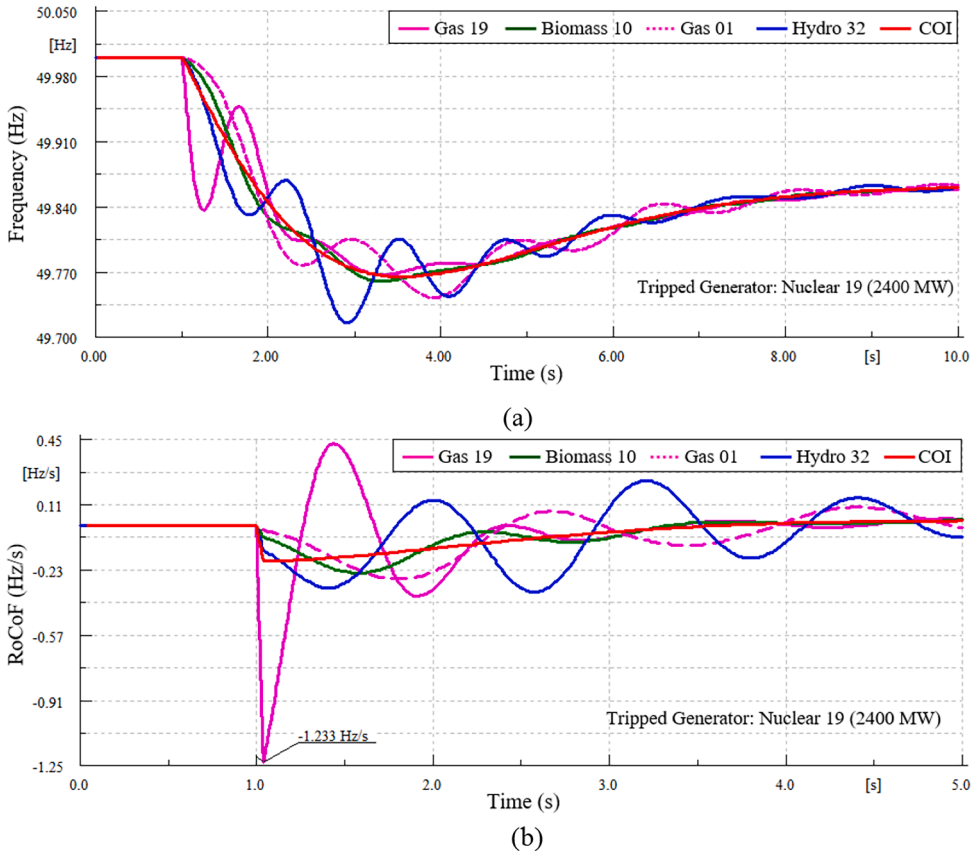

Fig. 11. 36-zone system frequency response to loss of 2400 MW generation: (a) the generators frequency and (b) the generators RoCoF.

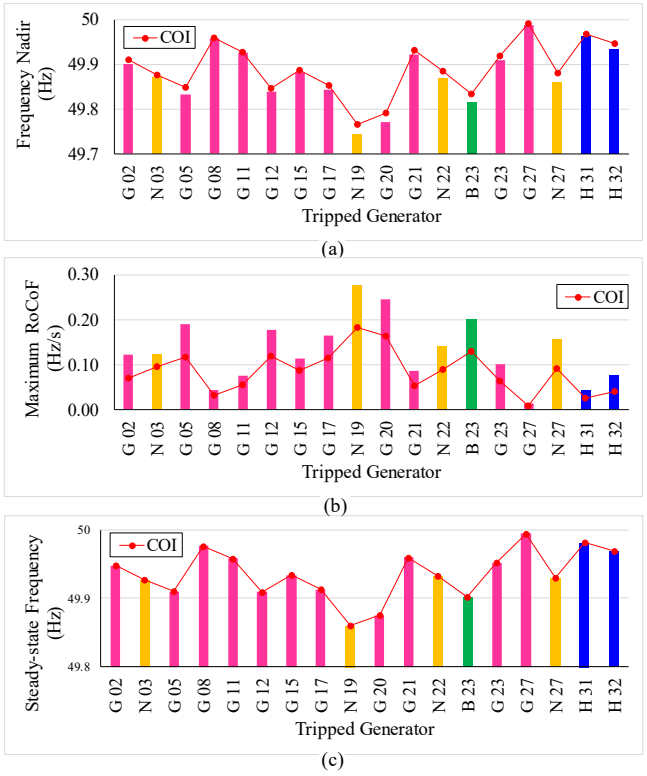

Fig. 12. Frequency control performance metrics measured in zone 1: (a) frequency nadir, (b) maximum RoCoF and (c) steady-state frequency.

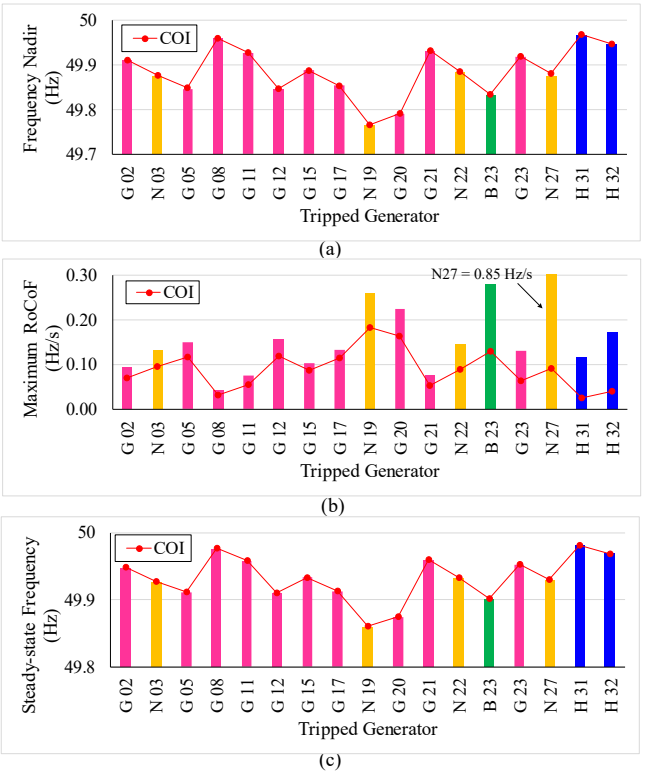

Fig. 13. Frequency control performance metrics measured in zone 27: (a) frequency nadir, (b) maximum RoCoF and (c) steady-state frequency.

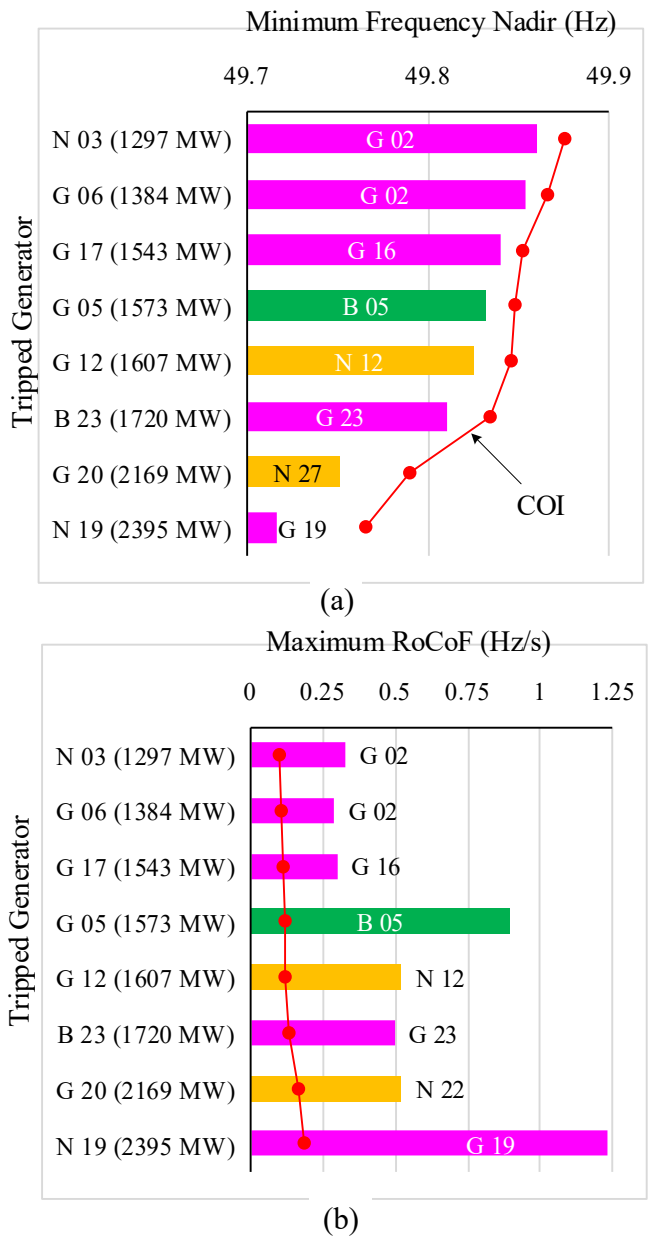

Fig. 14. Frequency control performance metrics of 36-zone power system: (a) minimum frequency nadir and (b) maximum RoCoF.

COI frequency nadir values increases with the loss of generation size. On the other hand, the local frequency gradients are always greater than the nation level COI RoCoF.

5. Conclusions

In this study, the frequency control performance of the Great Britain (GB) power system, which is reduced to 36-zone system, is investigated following the loss of generation contingencies. Initially, the researchers have developed illustrative dynamic models of the SGs exciter systems, thermal and hydro turbines as well as static Var compensators (SVCs) which are introduced into the network model for the purpose of frequency control studies. These are generically developed on the basis of the literature review and are not intended to be representative of specific generation connections within the NGESO GB master system. Further, the dynamic impact of these devices on small-signal stability and the system electromechanical modes in the frequency range of 0.5–1.25 Hz is examined using the modal analysis. It is observed that against the assumptions made, synchronous generators as modelled in the south eastern and south western parts of the 36-zone test system as well as the hydro units in the northern areas have the most influence on the slowest electromechanical modes. Furthermore, it is shown that the 36-zone system developed has the similar dynamic behavior with a single machine infinite bus system as the inertia of the SGs is increased. This can lead to the reduction of the electromechanical modes damping and their damped frequency. Conversely this alignment is reduced as the level of inertia and its location across the grid is varied. Moreover, it can be deduced that change of the inertia of the zones 1, 4, 10, and 32 is most effective and sufficient to control the damping of the slowest electromechanical modes. Afterward, the mode shape concept is employed, and it is observed that the first and second slowest modes of electromechanical mode groups are the inter-area modes and divides the 36-zone test system into two major parts which swings against each other. In this context, it is deduced that coast area in the southern part like zones 1, 3, 4, and 9 to 12 as well as the northern areas have the utmost contribution in the system frequency oscillations. Additionally, time-domain simulation studies are deployed to investigate the dynamic response of the developed test system following infeed loss incidents and validate the modal analysis results. It is to be noted that on the basis of the assumptions within the dynamic models the researcher has introduced, the maximum COI RoCoF is less than 0.25 Hz/s once the loss of generation is less than 2400 MW. Finally, we therefore have been able to illustrate how both national center assessment of frequency disturbances and its regional variation may be considered within a model capturing both generator dynamic assumptions and a sufficiently extensive network reduction of transmission system topology. Future works will extend the 36-zone test system to integrate dynamic modeling of renewable energy resources and battery energy storage systems.

CRediT authorship contribution statement

Rasoul Azizipanah-Abarghooee: Data curation, Writing – original draft, Software. **Mostafa Malekpour:** Conceptualization. **Mazaher Karimi:** Project administration, Validation. **Vladimir Terzija:** Supervision.

Declaration of Competing Interest

The authors declare that they have no known competing financial interests or personal relationships that could have appeared to influence the work reported in this paper.

Data availability

The authors do not have permission to share data.

Acknowledgment

The authors would like to thank National Grid ESO for providing the 36-zone GB power system reduction data as well as EFCC team for their insightful comments on the paper.

References

[1] Eto Joseph H. Use of frequency response metrics to assess the planning and operating requirements for reliable integration of variable renewable generation. Lawrence Berkeley National Laboratory; 2011.
[2] Milano F, Dörfler F, Hug G, Hill DJ, Verbič G. Foundations and challenges of low-inertia systems (Invited Paper). Power Syst Comput Conf (PSCC), Dublin 2018: 1–25.
[3] Future Energy Scenarios, National Grid ESO, [Online]. Available: https://www.nationalgrideso.com/future-energy/future-energy-scenarios.
[4] DeMarco FJ, Martins N, Ferraz JCR. An automatic method for power system stabilizers phase compensation design. IEEE Trans Power Syst 2013;28(2): 997–1007.

[5] Rostom D. Creation of a reduced model for the GB network. Warwick: National Grid ESO Draft Report; 2013.
[6] National Grid ESO, "National Grid ESO outline new approach to stability services in significant step forwards towards a zero-carbon electricity system," Warwick, 2020, [Online]. Available: https://www.nationalgrideso.com/news/national-grid-eso-outline-new-approach-stability-services-significant-step-forwards-towards.
[7] National Grid ESO, "Monthly balancing services summary 2020," National Grid ESO, Warwick, January 2020-V2, [Online]. Available: https://www.nationalgrideso.com/industry-information/industry-data-and-reports/system-balancing-reports.
[8] National Grid ESO, "Frequency response services", National Grid ESO, Warwick, January 2020-V2, [Online]. Available: https://www.nationalgrideso.com/industry-information/balancing-services/frequency-response-services.
[9] Canizares C, Fernandes T, Geraldi E, Gerin-Lajoie L, Gibbard M, Hiskens I, et al. Benchmark models for the analysis and control of small-signal oscillatory dynamics in power systems. IEEE Trans Power Syst 2017;32(1):715–22.
[10] IEEE Trans Power Syst, Feb 1992;7(1):37–44.
[11] Rogers G. Power System Oscillations. New York, NY, USA: Springer-Verlag; 2000.
[12] Demetriou P, Asprou M, Quiros-Tortos J, Kyriakides E. "Dynamic IEEE test systems for transient analysis. IEEE Syst J 2015.
[13] National Grid, Innovation, Enhanced frequency control capability project, [Online]. Available: http://www2.nationalgrid.com/UK/Our-company/Innovation/NIC/EFCC/.
[14] R. Azizipanah-Abarghooee, Wide-area monitoring based smart frequency control in future low-variable inertia systems with CCGT/wind/PV/BES/load, PhD Thesis, The University of Manchester (United Kingdom); 2019. [Online]. Available: https://www.research.manchester.ac.uk/portal/en/theses/widearea-monitoring-based-smart-frequency-control-in-future-lowvariable-inertia-systems-with-ccgtwindpvbesload(79eb04c3-5b5a-41b2-8d54-b20ecad1cb88).html.
[15] Malekpour M, Azizipanah-Abarghooee R, Teng F, Strbac G, Terzija V. Fast frequency response from smart induction motor variable speed drives. IEEE Trans Power Syst 2019;35(2):997–1008.
[16] Levi V, Williamson G, King J, Terzija V. Development of GB distribution networks with low carbon technologies and smart solutions: Methodology. Int J Electr Power & Energy Syst 2020;119:105833.
[17] Levi V, Williamson G, King J, Terzija V. Development of GB distribution networks with low carbon technologies and smart solutions: Scenarios and results. Int J Electr Power & Energy Syst 2020;119:105832.
[18] National Grid ESO, Electricity Ten Year Statement, [Online]. Available: https://www.nationalgrid.com/uk/publications/electricity-ten-year-statement-etys.
[19] MIGRATE Project, [Online]. Available: https://www.h2020-migrate.eu/.
[20] Phoenix Project, [Online]. Available: https://www.spenergynetworks.co.uk/pages/phoenix.aspx.
[21] P. Kundur, Power System Stability and Control, 1st Ed., Englewood Cliffs, NJ, U.S.A.: McGraw-Hill, Jan. 1994.
[22] "Load representation for dynamic performance analysis (of power systems)," *IEEE Trans. Power Syst.*, vol. 8, no. 2, pp. 472-482, May 1993.
[23] Price WW, Taylor CW, Rogers GJ. Standard load models for power flow and dynamic performance simulation. IEEE Trans Power Syst 1995;10(3):1302–13.
[24] Welfonder E, Weber H, Hall B. Investigations of the frequency and voltage dependence of load part systems using a digital self-acting measuring and identification system. IEEE Trans Power Syst 1989;4(1):19–25.
[25] C. Concordia and S. Ihara, "Load representation in power system stability studies," *IEEE Trans. Power App. Syst.*, vol. PAS-101, no. 4, pp. 969-977, Apr. 1982.
[26] Cheng M, Wu J, Galsworthy SJ, Ugalde-Loo CE, Gargov N, Hung WW, et al. Power system frequency response from the control of bitumen tanks. IEEE Trans Power Syst 2016;31(3):1769–78.
[27] DIgSILENT GmbH, "DIgSILENT PowerFactory Synchronous Machine Technical Reference Documentation," Tech. Rep. Revision 1, February 10, 2020.
[28] Malekpour M, Azizipanah-Abarghooee R, Zare M, Kiyoumarsi A, Terzija V. An explicit formulation for synchronous machine model in terms of the manufacturer data. Int J Electr Power & Energy Syst 2019;108:9–18.
[29] Krause P, Wasynczuk O, Sudhoff SD, Pekarek S. Analysis of electric machinery and drive systems. John Wiley & Sons; 2013.